Food Chemistry: X 27 (2025) 102448

Contents lists available at ScienceDirect

Food Chemistry: X

journal homepage: www.sciencedirect.com/journal/food-chemistry-x

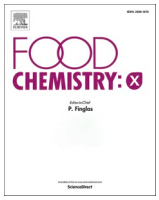

Sequential extraction of antioxidants from *Citrus aurantium* L. flower and kinetic evaluation of their effect on oil microparticle oxidative stability☆

Abdessamie Kellil [a], Rajat Suhag [a], Maria Concetta Tenuta [a], Sara Bolchini [a], Vakare Merkyte [b], Matteo Scampicchio [a], Ksenia Morozova [a], Giovanna Ferrentino [a,*]

[a] Faculty of Agricultural, Environmental and Food Sciences, Free University of Bolzano, Piazza Università, 1, Bolzano 39100, Italy
[b] Nestlé NPTC Waters, Via Dogana Vecchia snc, 24040 Madone, Italy

ARTICLE INFO

Keywords:
Supercritical fluid technologies
Ultrasound assisted extraction
Antioxidant activity
Encapsulation
Green technologies

ABSTRACT

This study applied supercritical CO_2 and ultrasound-assisted ethanol extraction (UAE) to obtain apolar and polar antioxidant fractions from *Citrus aurantium* flowers. HPLC-HRMS revealed distinct phytochemical profiles, with the polar extract showing higher phenolic content and antioxidant activity. Linseed oil was co-encapsulated with these extracts at varying concentrations (1, 2, and 5 mg/g of oil) using the Particles from Gas Saturated Solution (PGSS) technique, and the oxidative stability was assessed using isothermal calorimetry. Key kinetic parameters, such as induction time (τ), oxidation rates (R_{inh}, R_{uni}), and antioxidant efficiency (*A.E.*), were measured. The polar extract demonstrated superior *A.E.*, further confirmed by the DPPH stopped-flow assay. Co-encapsulation of both extracts produced an additive effect, surpassing the synthetic antioxidant BHT (200 μg/g). This study highlights *Citrus aurantium* flower extracts as natural antioxidants, enhancing the oxidative stability of encapsulated oils, while offering a sustainable method for bioactive compound recovery for food applications.

1. Introduction

Lipid oxidation is a primary factor in the degradation of vegetable oils and the decline of food products quality. This process leads to a reduction in nutritional value and the formation of harmful compounds, ultimately making the food unsuitable for consumption (Villeneuve et al., 2023). Microencapsulation is an established strategy for overcoming these challenges. This technology allows the formulation of unstable oily molecules into free-flowing and stable powders, reducing oxygen access and providing good oxidation protection for the oil (Reis et al., 2022). Although the encapsulation of oils provides a protective barrier through the wall material, the inclusion of specific additives, such as antioxidants, can further enhance the oxidative stability of oil and offer additional benefits in producing powders with diverse bioactive functionalities (Xiao & Ahn, 2023). Numerous studies have adopted this strategy, demonstrating significant improvements in the oxidative stability of encapsulated oils (Klettenhammer et al., 2023; Le Priol et al., 2021; Shehzad et al., 2021). However, shifting consumer preferences towards natural ingredients is putting pressure on the food industry to replace synthetic additives with natural alternatives. As a result, the search for novel antioxidants remains a significant area of research. In recent years, there has been a growing interest in investigating the antioxidant properties of natural compounds such as plant-based antioxidants and essential oils (Guo et al., 2021). These compounds not only have potential applications as new drugs or bioactive substances, but also could serve as safer alternatives to conventional synthetic antioxidants like butylated hydroxyanisole (BHA) and butylated hydroxytoluene (BHT), which are commonly used in processed food products (Baschieri et al., 2019).

Orange flowers (*Citrus aurantium* L. *Subsp. Amara L.*), have traditionally been valued for their pleasant aroma and used as a flavouring agent in foods and cosmetics (Farag et al., 2020). Recently, they have gained attention as a valuable source of bioactive compounds (Li et al., 2022; Ogunro et al., 2024). The essential oil derived from *C. aurantium* flowers is widely recognized for its potential to scavenge free radicals and prevent oxidative damage (de Sousa et al., 2023). However, beyond essential oils, *C. aurantium* flowers contain a range of antioxidant molecules, including both polar and apolar compounds, that contribute to its overall antioxidant potential. Examining both fractions is critical not only to gain a comprehensive understanding of the plant's antioxidant

☆ This article is part of a Special issue entitled: 'Plant-Based Products' published in Food Chemistry: X.

* Corresponding author.
E-mail address: giovanna.ferrentino@unibz.it (G. Ferrentino).

https://doi.org/10.1016/j.fochx.2025.102448
Received 1 November 2024; Received in revised form 2 March 2025; Accepted 7 April 2025
Available online 8 April 2025
2590-1575/© 2025 Published by Elsevier Ltd. This is an open access article under the CC BY-NC-ND license (http://creativecommons.org/licenses/by-nc-nd/4.0/).

capabilities, but also to discover its full potential as a natural source of bioactive compounds.

While the importance of extracting both polar and apolar antioxidants is clear, traditional extraction methods such as hydrodistillation and solvent extraction often fail to effectively obtain these diverse compounds (Lefebvre et al., 2021). These conventional techniques are typically limited by their inability to efficiently extract both types of antioxidants simultaneously, leading to partial recovery of the bioactive compounds (Pereira et al., 2019). Furthermore, they often involve high temperatures and long processing times, which can degrade sensitive compounds, compromising the quality and antioxidant capacity of the extracts (Daud et al., 2022). Advanced extraction techniques such as supercritical CO_2 (SC-CO_2) extraction and ultrasound-assisted extraction (UAE) offer promising alternatives. SC-CO_2 is particularly effective for isolating apolar, thermolabile compounds under mild conditions, preserving their bioactivity (Ferrentino et al., 2018). In contrast, UAE with ethanol as a solvent excels in extracting polar compounds, improving both extraction efficiency and reducing processing time (Allay et al., 2024; Gasparini et al., 2023). When engaged sequentially, these two methods complement each other, enabling the targeted recovery of both apolar and polar fractions and thereby offering a more complete and robust antioxidant profile from the plant.

Therefore, this study aims to determine the antioxidant efficiency of the polar and apolar fractions of *C. aurantium* flowers in enhancing the oxidative stability of encapsulated linseed oil. To explore the impact of composition and functionality in greater depth, the orange flowers underwent a two-step exhaustive extraction process. SC-CO_2 was first employed to recover the apolar fraction. The residue was then extracted with ethanol using ultrasound-assisted extraction (UAE) to obtain the polar fraction. Both extracts (individually and mixed at equal concentrations) were subsequently added to linseed oil and encapsulated using the particles from gas saturated solutions (PGSS) technique. This is a supercritical CO_2-based encapsulation technology operating at relatively low temperatures and in an oxygen-free environment, suitable for heat sensitive compounds like oils. Isothermal calorimetry was then employed to assess the oxidation kinetics. The antioxidant efficiency of both extracts was also compared with that of a synthetic antioxidant (BHT). By demonstrating the potential of both apolar and polar extracts to enhance the oxidative stability of encapsulated linseed oil, this study contributes to the valorisation of underutilized plant materials and offers novel insights into their antioxidant potential.

2. Materials and methods

2.1. Materials

Linseed oil and carnauba wax were purchased from Sigma-Aldrich (Milano, Italy). Orange flowers (*Citrus aurantium* L. *Subsp. Amara L.*) were kindly donated by Nestlé spa (Bergamo, Italy). All other chemicals used in this study were of analytical grade and obtained from Sigma-Aldrich (Milano, Italy).

2.2. Extraction procedure

2.2.1. Supercritical CO_2 extraction

Apolar fraction of *C. aurantium* flowers was extracted using a SC-CO_2 system (Superfluid s. r.l, Padova, Italy), following a procedure described by Jokić et al. (2016). The dried plant material (180 g) was ground using a hammer miller (Mill-LM3100, Perten Instruments, Sweden) equipped with 800 μm mesh size, and sieved (Retsch GmbH, Verder Scientific, Germany) to yield an average particle size distribution of 7.7 % with a diameter between 500 μm and 1000 μm, 26 % - 250 to 500 μm, 35.6 % - 100 to 250 μm, and 30.6 % $<$ 100 μm. The plant powder obtained was loaded in a stainless-steel extraction cell of 800 mL volume. The extraction cell was then placed inside the extractor chamber. The extraction was performed in duplicates at a constant temperature (40 °C) and pressure (20 MPa), with a CO_2 flow rate of 1 L/h for 90 min. The apolar extracts were collected and stored under nitrogen at −80 °C until analysis. The yield was calculated as a percentage of the ratio of the amount (g) of extract and the mass (g) of powdered material used for the extraction.

2.2.2. Ultrasound assisted extraction

UAE was performed using an ultrasonic system (Hielscher UP400st, 400 W and 24 kHz, Hielscher Ultrasonic GmbH, Teltow, Germany), equipped with a 22 mm diameter titanium sonotrode, following a procedure described by Zhang et al. (2023) with some modifications. In a glass flask, 10 g of the *C. aurantium* flowers solid residue obtained after supercritical CO_2 extraction were mixed with 100 mL of ethanol, as shown in supporting information, Fig S1. The sonotrode was immersed in the extraction solvent. The extraction was carried out at 75 W (60 % amplitude) for 40 min. The top of the flask was covered with an aluminium foil to minimize solvent evaporation during extraction. The temperature was continuously monitored by a digital thermometer and controlled at 30 ± 2 °C in an ice bath to limit sample oxidation. The extract was then filtered through a Watman filter paper and the solvent was evaporated in a rotary evaporator under vacuum (LABOROTA 4000, Heidolph, Schwabach, Germany) at 35 °C. The obtained extracts were weighed and stored at −80 °C for further analyses. The yield of UAE was expressed as (g) of dry extract per (100 g) of sample used for the extraction.

2.3. Characterization of *C. aurantium* flower extracts

2.3.1. Total phenolic content

Total phenolic content (TPC) was determined spectrophotometrically using the Folin-Ciocalteu colorimetric method (Singleton & Rossi, 1965). For the apolar fraction, phenolic compounds were first extracted using methanol as a solvent, via a liquid-liquid extraction (Siger et al., 2008). Meanwhile, the polar extract was directly reconstituted in methanol to a known concentration before analysis. In brief, 130 μL of the diluted extracts were mixed with 1 mL of Milli-Q water and 130 μL of Folin-Ciocalteu reagent. After 5 min, 130 μL of Na_2CO_3 (20 % *w/v*) was added, and the mixture was incubated in the dark at room temperature for 2 h. The absorbance was recorded at 765 nm with a UV–Vis spectrophotometer (Cary 100 Series, Agilent Technologies, Italy), and the total phenolic content values were expressed as gallic acid equivalents (mg GAE g^{-1} of dry extract).

2.3.2. Classical DPPH assay

The antioxidant capacity was assessed using classical DPPH assay (Brand-Williams et al., 1995). For the analysis, 0.5 mL of *C. aurantium* flower extracts were added to 0.5 mL of DPPH solution (200 μM in methanol) and mixed. Then, the samples were incubated for one hour in the dark, and the absorbance was measured at 515 nm using a UV–Vis (Cary 100 Series, Agilent Technologies, Italy). The DPPH antioxidant capacity was calculated from the Trolox (6-hydroxy-2, 5, 7, 8-tetramethylchroman-2-carboxylic acid) calibration curve. The results were expressed as μmol Trolox equivalent per g of dry extract.

2.3.3. DPPH stopped-flow kinetic

A kinetic-based DPPH method was performed with a stopped-flow system (RX2000, Applied Photophysics, Leatherhead, UK) equipped with a pneumatic pump, a quartz flow-cell mounted on a Cary 60, UV–VIS spectrophotometer (Agilent Technology, Santa Clara, CA, USA). The stopped-flow system had two syringes, one loaded with a methanolic (200 μM) DPPH solution, and the other with a standardized concentration (60 μM GAE) of *C. aurantium* flowers extracts as determined by Folin-Ciocalteu assay. As soon as the pneumatic drive was pressed, equal volumes of the two solutions were mixed and transferred into the quartz flow cell. The resulting absorbance of the reaction mixture was recorded every 20 ms at a wavelength of 515 nm. The

concentration of the DPPH was calculated from the recorded absorbance signal by applying the Beer-Lambert law. Simulation and fitting of the reaction kinetic data, as well as optimal values of rate constants of main reaction (k_1) and side reaction (k_2) were obtained using the software Copasi (version 4.29) as described in Angeli et al. (2023). Simulated DPPH consumption was obtained from solving a set of differential equations derived by the law of mass action applied to eqs. 1 and 2.

$$AH + DPPH\bullet \xrightarrow{k_1} A\bullet + DPPH - H \quad (1)$$

$$A\bullet + DPPH\bullet \xrightarrow{k_2} \text{Products} \quad (2)$$

where, AH - antioxidant, and A• - oxidized form of the antioxidant. Optimal values of the rate constants (k_1 and k_2) were determined by minimizing, through iteration, the sum of squared errors between the experimental and simulated data. The measurements were performed in triplicates.

2.3.4. Ferric reducing antioxidant power (FRAP) assay

The reducing capacity of the extracts was estimated by the FRAP assay. The method is based on the reduction of the ferric 2,4,6-tripyridyl-*s*-triazine complex (Fe^{+3}-TPTZ) to its ferrous, blue-colored form (Fe^{+2}-TPTZ) by antioxidants present in the sample (Benzie & Strain, 1996). The FRAP reagent was freshly prepared by combining acetate buffer (pH 3.6), ferric chloride solution (20 mM), and TPTZ solution (40 mM in 40 mM hydrochloric acid) in a ratio of 10:1:1 (*v*/v/v). For the analysis, an aliquot of 10 µL of extracts solutions (1 mg/mL) was mixed with 190 µL of FRAP reagent, and the mixture was incubated at room temperature for 30 min. The absorbance was then measured at 593 nm using a spectrophotometer (Tecan, Infinite M Nano+, Switzerland). A calibration curve was constructed with Trolox (6-hydroxy-2, 5, 7, 8-tetramethylchroman-2-carboxylic acid) and the results were expressed as µmol Trolox equivalent per g of dry extract.

2.3.5. ABTS assay

The ABTS (2,2′-Azino-bis (3-ethylbenzothiazoline-6-sulfonic acid)) radical scavenging assay was used to determine the antioxidant activity of the samples by measuring their ability to neutralize the $ABTS^{+}\bullet$ cation radical (Charles, 2013). The radical was generated through the reaction between ABTS (7 mM) and potassium persulfate (2.45 mM) in an equal-volume mixture, which was incubated in the dark for 24 h at room temperature. This process resulted in a stable blue-green solution with an absorbance value between 0.7 and 0.8 at 734 nm, confirmed using a UV–Vis spectrophotometer (Cary 100 Series, Agilent Technologies, Italy). To perform the assay, aliquots of 50 µL of the extracts (1 mg/mL) were added to 1 mL of the $ABTS^{+}\bullet$ solution, and the mixture was incubated in the dark for 10 min. The absorbance of the reaction mixture was recorded at 734 nm, and the antioxidant activity was quantified by comparison to Trolox (6-hydroxy-2, 5, 7, 8-tetramethylchroman-2-carboxylic acid) standard curve. Results were expressed as µmol Trolox equivalent per g of dry extract.

2.3.6. Characterization of extracts by liquid chromatography

Extracts obtained from SC-CO_2 and UAE extractions were analysed using HPLC coupled with a high-resolution mass spectrometer (HRMS). The analysis was performed using an Ultimate 3000 UHPLC instrument coupled with diode array detector (DAD) and Q-Exactive Orbitrap HRMS detector (Thermo Fisher Scientific, USA). For the SC-CO_2 extract, a Kinetex F5 column (150 × 4.6 mm, 2.6 µm particle size, Phenomenex, CA, USA) was utilized for the analysis, while a Kinetex Biphenyl column (100 × 2.1 mm, 2.6 µm particle size, Phenomenex, CA, USA) was used for the UAE extract. The temperature of the column was kept constant at 30 °C. The mobile phases used were Milli-Q water with 0.5 % acetic acid (*v*/v) (A) and methanol with 0.5 % acetic acid (v/v) (B). Before injection, the samples were filtered using 0.22 µm pore size filters, and the injection volume was set at 20 µL. For the SC-CO_2 extract, a flow rate of 1.2 mL/min was used with the following gradient for optimal chromatographic separation: from 0 to 1 min with 75 % of eluent B; from 1 to 15 min with a increasing of eluent B until 95 %; hold 2 min at 95 %, after in 1 min arrive at 100 %, hold until 23 min at 100 %, from 23 to 24 min with a decreasing % of eluent B from 100 % to 75 %; re-equilibration for 6 min. A flow rate of 0.3 mL/min was used for the UAE extract, following a gradient: from 0 to 2 min with 5 % of eluent B; from 8 to 11 min with 30 % of eluent B; from 31 to 34 min with 90 % of eluent B; from 34 to 41 min with a decreasing % of eluent B from 90 % to 5 %; from 41 to 45 min with 5 % of eluent B. MS analysis operated in both positive and negative ion mode with ultrapure nitrogen as sheath (20 arb), and auxiliary (5 arb) gas (250 °C). The capillary voltage was maintained at 4.5 kV, while the capillary temperature was set at 320 °C. The full MS scans ranged from 50 to 750 *m/z* for the UAE extract and 100 to 1000 *m/z* for the SC-CO_2 extract, both with a resolution of 70,000, AGC target of 3×10^6, and maximum injection time of 100 ms. The dd-MS/MS settings were as follows: AGC target 5×10^5 for the SC-CO_2 extract and 1×10^5 for the UAE extract, with a resolution of 17,500, maximum injection time of 50 ms, and isolation window of 4.0 m/z. MS data were collected and analysed using Xcalibur 3.1 and Compound Discoverer 3.3 software (Thermo Fisher Scientific, USA).

2.4. Co-encapsulation of linseed oil and C. aurantium flower extracts by PGSS

Carnauba wax, a food grade and natural lipid carrier, was selected for its good thermal stability and compatibility with oil-based formulations. Its ability to solubilize and melt in CO_2 under mild conditions makes it suitable for the PGSS process. An oil-to-wall material ratio of 1:5 was chosen based on preliminary experiments. Microparticle production was carried out using a PGSS system (Superfluidi s.r.l., Padova, Italy), which consists of 500 mL high-pressure vessel and an expansion chamber operating at ambient temperature and pressure. The vessel temperature was automatically controlled by a thermostatic water bath. The CO_2 was cooled to 4 °C (Euroklima R407C, Siziano, Italy) and pumped to the high-pressure vessel via a diaphragm pump (Lewa LDC e M e 9XXV1, Milano, Italy). The desired formulation was prepared by mixing 2 g of linseed oil and 8 g of carnauba wax. Extracts obtained from *C. aurantium* flowers were added to the oil at different concentrations (1 mg/g, 2 mg/g, and 5 mg/g). The oil-carrier mixture was then loaded into the high-pressure reactor, which was sealed and saturated with CO_2. The working conditions of temperature (80 °C) and pressure (10 MPa) were determined based on preliminary experiments, which indicated that the selected settings allowed the formation of a saturated solution in supercritical CO_2. The formulation remained in the reactor under these conditions for 30 min before depressurization through a 1000 µm nozzle. The resulting microparticles were collected and stored in amber vials under nitrogen. The physico-chemical properties of the obtained microparticles including the encapsulation efficiency, bulk and tapped density, flowability, particle size distribution, and morphology are described in the Supporting information.

2.5. Oxidative stability of microparticles

The oxidative stability of linseed oil microparticles was assessed using isothermal calorimetry (Thermal Activity Monitor Model 421 TAM III, TA Instruments, Milan, Italy). The experimental procedure followed the one reported by Klettenhammer et al. (2023). Experiments were conducted at a constant temperature of 40 °C. This temperature allowed the assessment of the oxidative stability of samples having long-term stability under accelerated storage (Rahmania et al., 2020). Each sample, precisely weighed to 100 ± 1 mg, was carefully loaded into a 4 mL hermetically sealed glass ampoule. The generated heat flow signal was then continuously monitored over time.

2.6. Determination of kinetic parameters of oxidation

Lipid oxidation typically involves the formation (initiation, eq. 3), propagation (eq. 4 and 5), and termination (eq. 6) of lipid radicals. These reactions occur simultaneously and are characterized by defined rate constants (Farhoosh, 2022):

Initiation:

$$LH \xrightarrow{R_i} L\bullet + H\bullet \tag{3}$$

Propagation:

$$L\bullet + O_2 \xrightarrow{R_0} LOO\bullet \tag{4}$$

$$LH + LOO\bullet \xrightarrow{k_p} LOOH + L\bullet \tag{5}$$

Termination:

$$2LOO\bullet \xrightarrow{k_t} NRP \tag{6}$$

The initiation step involves a hydrogen atom abstraction from an unsaturated lipid (LH), leading to the formation of an alkyl radical $L^{\bullet}$, which reacts rapidly with O_2 to generate peroxyl radicals. The rate of initiation can be determined using eq. (7) (Suhag et al., 2025):

$$R_i = \frac{n \times [AH]}{\tau} \tag{7}$$

where τ is the induction time in the presence of a known concentration of a reference antioxidant with well-known stoichiometric factor (n). For this, linseed oil microparticles were prepared by adding 30 μM concentration of α-tocopherol [AH] with $n = 2$ which provided an induction time (τ) = 63.3 ± 2.2 × 10^4 s leading to a rate of initiation R_i equal to 9.5 ± 0.5 × 10^{-11} M·s^{-1}.

Then, the peroxyl radical reacts with an unsaturated lipid to generate a lipid peroxide and a new alkyl radical. These reactions are referred to as propagation because each reaction generates a new radical and maintains the chain of reactions. Finally, two peroxyl radicals may react and form a non-radical product (NRP).

To determine the kinetic parameters related to the microparticles oxidation, the calorimetric traces were first transformed to conversion fraction (α) calculated by dividing the accumulated heat (i.e., cumulative integration of the heat flow rate) by the overall heat (Q_{tot}), as defined in eq. 8 (Suhag et al., 2025):

$$\alpha = \frac{\int_0^t \dot{q}.dt}{Q_{tot}} \tag{8}$$

Next, from the conversion fraction values it was possible to derive the oxygen consumed during the oxidation using the following equation (Suhag et al., 2025):

$$[O_2]_t = \left(\frac{V_H}{V_S}\right) \times \frac{P_{O_2}}{R \bullet T} \times [1 - \alpha(t)] \tag{9}$$

where, V_H = 3.4 cm^3, and V_S = 0.6 cm^3 are the volumes of headspace and sample inside the ampoule, respectively. P_{O2} = 0.21 atm, T = 313 K, and R = 0.082 L atm/K mol.

The rate of peroxidation (R_{uni}) is given by eq. (10) (Suhag et al., 2025), if the rates of formation for the radical species R• and ROO• are set to zero (Cosgrove et al., 1987):

$$R_{uni} = \frac{-d[O_2]_{uni}}{dt} = \frac{k_p}{\sqrt{2k_t}} \times [RH] \times \sqrt{R_i} \tag{10}$$

where, $[O_2]$ and [RH] are the oxygen and lipid substrate molar concentrations, respectively. The ratio $k_p/\sqrt{2k_t}$ represents the oxidizability index (*O.I.*) given by the following equation (Suhag et al., 2025):

$$O.I. = \frac{k_p}{\sqrt{2k_t}} = \frac{R_{uni}}{[RH] \times \sqrt{R_i}} \tag{11}$$

here, k_p and k_t are the rate constants of the propagation and termination reactions, respectively. In the presence of chain breaking antioxidants, the lipid oxidation can be effectively controlled by reacting with peroxyl radicals following the scheme:

Inhibition:

$$LOO\bullet + AH \xrightarrow{k_{inh}} LOOH + A\bullet \tag{12}$$

$$LOO\bullet + A\bullet \xrightarrow{k_A} NRP \tag{13}$$

The relationship between the rate of the inhibited period (R_{inh}) and the rate of initiation (R_i) is given by eq. (14):

$$R_{inh} = \frac{-d[O_2]_{inh}}{dt} = \frac{k_p}{k_{inh}} \times \frac{[RH] \times R_i}{n \times [AH]} \tag{14}$$

where, k_{inh} is the rate constant of the inhibition step, and the ratio k_{inh}/k_p stands for the antioxidant efficiency (*A.E.*, eq. 15), reflecting the competition between the eqs. (5) and (12). The higher the *A.E.*, the greater is the efficiency of the antioxidant in inhibiting the lipid peroxidation reaction. Assuming R_i remains constant for all microparticles, *A.E.* can be obtain using the following equation (Pryor et al., 1993):

$$A.E. = \frac{k_{inh}}{k_p} = \frac{R_i}{n \times [AH]_0} \times \frac{[RH]_0}{\tau \times R_{inh}} \tag{15}$$

2.7. Statistical analysis

The experimental measurements were performed in triplicate and expressed as mean ± standard deviation. One-way ANOVA followed by Tukey's test was used to check differences between mean values. The significance of differences was defined at the $p < 0.05$ level. Figures were prepared using OriginPro 2021 (version 9.8.0.200), OriginLab Corporation, USA.

3. Results and discussion

3.1. Total phenolic content and antioxidant activity

Table 1 presents the results of TPC, FRAP, ABTS and classical DPPH assays, as well as stopped-flow DPPH kinetics for both the apolar and polar extracts of *C. aurantium* flowers. The polar extract exhibited a significantly ($p < 0.05$) higher TPC value (70.11 ± 3.25 mg GAE ·g^{-1} of dry extract) compared to the apolar extract (8.95 ± 1.14 mg GAE·g^{-1} of dry extract). This finding was consistent with Değirmenci and Erkurt (2020), who reported a TPC value of 81.37 ± 3.2 mg GAE·g^{-1} for the ethanolic extract of *C. aurantium* flowers, which was much higher than the 1.54 ± 0.08 mg GAE·g^{-1} observed in the essential oil fraction. Degirmenci and Erkurt (2020) also highlighted the significant impact of solvent polarity on phenolic content in *C. aurantium* flowers. Methanolic extracts exhibited the highest TPC (87.96 ± 3.15 mg GAE·g^{-1}), while nonpolar solvents like hexane yielded considerably lower values (27.12 ± 2.46 mg GAE·g^{-1}). Similarly, comparable TPC values have been reported for other citrus flower extracts, including *Citrus aurantium* (78.76 mg GAE·g^{-1} of extract), *Citrus sinensis* (78.47 mg GAE·g^{-1} of extract), *Citrus nobilis* (62.10 mg GAE·g^{-1} of extract), and *Citrus limon* (60.01 mg GAE·g^{-1} of extract) (Nabavi et al., 2016). The higher TPC value in the polar extract can be attributed to the ethanol's ability to form hydrogen bonds with phenolic compounds, enhancing their solubility and extractability (Gil-Martín et al., 2022). In contrast, the lower TPC value in the apolar SC-CO_2 extract is consistent with the limited capacity of supercritical CO_2 to extract polar compounds (Klein et al., 2019).

The antioxidant activity of the extracts was assessed using FRAP,

Table 1
Results of total phenolic content (TPC), classical DPPH assay, and kinetic stopped-flow DPPH method, FRAP and ABTS assays on *C. aurantium* flower extracts.

Extract	Yield	TPC	FRAP	ABTS	Classical DPPH	DPPH kinetic	
	(*w*/w %)	GAE (mg•g^{-1})	TE (μmol•g^{-1})	TE (μmol•g^{-1})	TE (μmol•g^{-1})	k_1 (M^{-1} s^{-1})	k_2 (M^{-1} s^{-1})
Apolar	2.4 ± 0.4^{b}	8.95 ± 0.17^{b}	24.32 ± 2.30^{b}	66.45 ± 1.25^{b}	6.13 ± 0.12^{b}	903.94 ± 57.69^{b}	67.59 ± 0.07^{a}
Polar	13.6 ± 1.2^{a}	70.11 ± 0.32^{a}	208.32 ± 3.98^{a}	103.95 ± 1.62^{a}	44.58 ± 3.04^{a}	1388.87 ± 91.17^{a}	85.91 ± 7.84^{a}

Values are presented as mean ± standard deviation ($n = 3$). Values with different letters in the same column are significantly different ($p < 0.05$).
(k_1): rate constant of the main reaction between antioxidants and DPPH, and (k_2): rate constant of the side reaction.

ABTS, and DPPH assays (Table 1). FRAP assay revealed a significantly higher reducing power for the polar extract (208.32 ± 3.98 μmol TE·g^{-1}) compared to the apolar extract (24.32 ± 2.30 μmol TE·g^{-1}). Similarly, the ABTS assay indicated higher antioxidant activity for the polar fraction (103.95 ± 1.62 μmol TE·g^{-1}) relative to the apolar fraction (66.45 ± 1.25 μmol TE·g^{-1}).

When compared to other flower extracts, the polar fraction of *C. aurantium* flower exhibited higher FRAP and ABTS values than those reported for *Calendula officinalis* L. (FRAP = 58 μmol TE·g^{-1}; ABTS = 71 μmol TE·g^{-1}), *Gomphrena globosa* Linn. (FRAP = 8 μmol TE·g^{-1}; ABTS = 46 μmol TE·g^{-1}), and *Jasminum sambac* (L.) Ait (FRAP = 48 μmol TE·g^{-1}; ABTS = 97 μmol TE·g^{-1}). However, these values were lower than those reported for *Rosmarinus officinalis* L. and *Perennial chamomile* flowers (Chen et al., 2015). The observed antioxidant activity is likely attributed to the phenolic compounds present in the extracts, as their hydroxyl groups are known to play a key role in radical scavenging. A positive correlation between total phenolic content and antioxidant activity was also confirmed in this study.

In the classical DPPH assay, the polar extract showed significantly higher scavenging activity than the apolar extract ($p < 0.05$) (Table 1). Its antioxidant activity surpassed that of *Gomphrena globosa* Linn. flowers but was lower than that of *Rosmarinus officinalis* L. and Perennial chamomile flowers (Chen et al., 2015). To evaluate in-depth the rate at which antioxidants in the extract neutralize the radicals, the DPPH stopped-flow kinetic assay was tested. The polar extract demonstrated a significantly higher antioxidant reactivity, as indicated by a higher rate constant ($k_1 = 1388.87 \pm 91.17$ M^{-1} s^{-1}) compared to the apolar extract ($k_1 = 903.94 \pm 57.69$ M^{-1} s^{-1}) (Fig. 1, Table 1). These rate constants showed a strong correlation with the TPC values of the extracts and are consistent with the findings of Angeli et al. (2023). The higher reactivity of the polar extract can be explained by its extraction method (UAE-ethanol), which effectively extracts polar antioxidants, such as phenols,

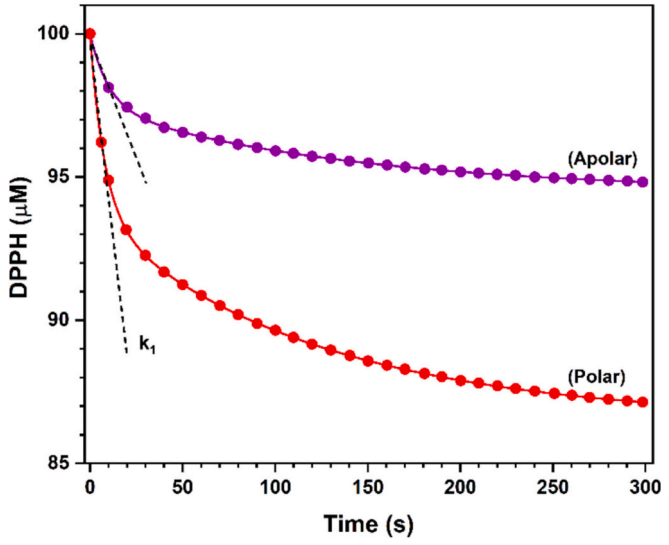

Fig. 1. Kinetic curves and fittings of the reaction between 100 μM of DPPH• with apolar, and polar *Citrus aurantium* L. *Subsp. Amara* L. flower extracts standardized to 30 μM GAE.

known for their strong antioxidant properties. The significant influence of the extraction solvent on both phenolic content and antioxidant activity was also demonstrated by Park et al. (2014) in orange flesh and peel.

3.2. Phytochemical profile of polar and apolar C. aurantium flower extracts

To further understand and validate the antioxidant assay results of the two extracts, a characterization of the compounds potentially responsible for their antioxidant activity was performed using HPLC-HRMS. Fig S2 (supporting information) shows the chromatograms with the identification of the main detected compounds listed in Tables 2 and 3 for apolar and polar extracts, respectively. As expected, the phytochemical profiles of the extracts were markedly different. The SC-CO_2 extract was dominated by non-polar compounds, including quinine (39.6 %), isocaffeine (15.7 %), and polymethoxylated flavones (PMFs) such as tangeretin (~10 %), nobiletin (~9 %), and 5,6-dihydroxy-7,8,3′,4′-tetramethoxyflavone (~4.4 %). It also contained the coumarin bergapten (1.4 %), as well as notable levels of tocopherols (~11 %) and tocotrienols (>1 %).

In contrast, the UAE extract was rich in polar *Citrus* flavanones, including hesperetin (46.7 %) and its glucosidic derivative hesperetin 7-glucoside (3.9 %), along with naringenin (24.6 %), hesperidin (3.7 %), and neoeriocitrin (2.8 %). The high concentration of these flavanones, particularly hesperetin and naringenin, is likely responsible for the superior antioxidant activity. These compounds, well-documented as potent free radical scavengers, contain hydroxyl groups capable of donating hydrogen atoms to neutralize radicals (Wang et al., 2022), thereby contributing to the higher antioxidant capacity and faster reaction rates in the classical and kinetic DPPH assay, respectively. Additionally, the presence of quinic acid (9.2 %), known for its antioxidant properties (Legua et al., 2022), may enhance the overall activity of the polar extract. It is also important to highlight the potential synergistic effects of these compounds. The combination of flavonoids like hesperetin and naringenin may improve the stability and efficacy of radical scavenging. The synergistic action between phenolic acids, flavonols, and flavanones could also contribute to the enhanced activity, as observed in other studies performed on citrus-based extracts (Freeman et al., 2010). This potential synergy highlights the complexity of the antioxidant behaviour in multi-compound mixtures, where the whole extract activity can surpass that of individual compounds.

3.3. Antioxidant effect of C. aurantium flower extracts on the oxidative stability of linseed microparticles

The antioxidant efficiency (*A.E.*) of both the apolar and polar *C. aurantium* flower extracts in improving the oxidative stability of linseed oil microparticles was investigated. For this purpose, the *C. aurantium* flower extracts were incorporated and co-encapsulated with linseed oil using the PGSS technique. Oxidation kinetics was determined using a previously validated isothermal calorimetry approach (Klettenhammer et al., 2023; Suhag, Ferrentino, et al., 2024) at 40 °C. This technique allowed for real-time measurement of the heat flow associated with oxidation reactions in the oil microparticles, providing simultaneous kinetic data on antioxidant activity and

Table 2
Phytochemical composition of *C.aurantium* flowers SC-CO_2 (apolar) extract.

Peak	Compound	Rt (min)	Formula	Adduct	*m/z* theoretical	*m/z* measured	Δ (ppm)	MS/MS	Area (%)
1	Isocaffeine	1.61	$C_8 H_{10} N_4 O_2$	$[M + H]^+$	195.0876	195.08757	−0.40		15.71 ± 0.03
2	Trans cinnamic acid	1.8	$C_9 H_8 O_2$	$[M\text{-}H]^-$	147.0451	147.0451	−0.03	99.0816	2.37 ± 0.02
3	2-tert-Butyl-4-methoxyphenol	2.24	$C_{11} H_{16} O_2$	$[M + H]^+$	181.1223	181.1220	−0.63	163.1116, 135.1167	0.15 ± 0.01
4	Albaflavenol	2.37	$C_{15} H_{24} O$	$[M + H]^+$	221.1899	221.18985	−0.28	203.1795, 111.1168	0.04 ± 0.01
5	Apigenin	2.46	$C_{15} H_{10} O_5$	$[M\text{-}H]^-$	269.0455	269.0456	0.42		0.10 ± 0.01
6	Bergapten	2.77	$C_{12} H_8 O_4$	$[M + H]^+$	217.04950	217.04925	−1.31	217.0494, 202.0261	1.41 ± 0.02
7	Tangeretin	3.08	$C_{20} H_{20} O_7$	$[M + H]^+$	373.12818	373.12821	0.08	343.0815, 373.1284, 358.1048	9.98 ± 0.03
8	Nobiletin	3.96	$C_{21} H_{22} O_8$	$[M + H]^+$	403.13874	403.13849	−0.64	373.0919, 403.1389, 388.1154	9.10 ± 0.02
9	5,6-Dihydroxy-7,8,3′,4′-tetramethoxyflavone	4.20	$C_{19} H_{18} O_8$	$[M + H]^+$	375.10744	375.10729	−0.42	343.0813, 373.1283, 358.1047	4.38 ± 0.01
10	Quinine	5.56	$C_{20} H_{24} N_2 O_2$	$[M + H]^+$	325.1910	325.1908	−0.52	307.1805, 264.1383, 253.1335	39.62 ± 0.03
11	Trans-10-heptadecenoic acid	8.87	$C_{17} H_{32} O_2$	$[M\text{-}H]^-$	267.2329	267.2328	−0.32		1.34 ± 0.01
12	alpha tocotrienol	9.45	$C_{29} H_{44} O_2$	$[M + H]^+$	425.34141	425.34186	0.54	365.1936, 281.1362	0.20 ± 0.01
13	gamma tocotrienol	10.06	$C_{28} H_{42} O_2$	$[M + H]^+$	411.32576	411.32563	−0.31	150.0915	0.29 ± 0.01
14	delta-tocopherol	14.64	$C_{27} H_{46} O_2$	$[M + H]^+$	403.3570	403.3570	0.40	137.0600, 105.0701	3.78 ± 0.03
15	beta-tocopherol	15.23	$C_{28} H_{48} O_2$	$[M + H]^+$	417.3727	417.3727	0.01	135.1169, 107.0856	3.03 ± 0.01
16	gamma-tocopherol	15.60	$C_{28} H_{48} O_2$	$[M + H]^+$	417.3727	417.3727	0.02	135.1168, 107.0862	1.59 ± 0.02
17	Sitosterol	15.86	$C_{29} H_{50} O$	$[M + H\text{-}H_2O]^+$	415.3934	397.3829	0.03	397.3842, 161.1327, 147.1161	0.40 ± 0.01
18	alpha-tocopherol	16.21	$C_{29} H_{50} O_2$	$[M + H]^+$	431.3883	431.3883	0.01	165.0914	2.53 ± 0.02

Table 3
Phytochemical composition of *C. aurantium* flowers UAE ethanolic (polar) extract.

Peak	Compound	Rt (min)	Formula	Adduct	*m/z* theoretical	*m/z measured*	Δ (ppm)	MS/MS	Area (%)
1	D-(−)-Quinic acid	1.02	$C_7 H_{12} O_6$	$[M\text{-}H]^-$	191.0561	191.0559	−1.27	85.0294	9.20 ± 0.02
2	Pyrogallol	1.53	$C_6 H_6 O_3$	$[M + H]^+$	127.0389	127.0390	0.52	109.0285, 81.0336	0.41 ± 0.01
3	Chlorogenic acid	9.43	$C_{16} H_{18} O_9$	$[M + H]^+$	355.1023	355.1028	1.20	163.0392	0.47 ± 0.01
4	Eriodictyol	18.26	$C_{15} H_{12} O_6$	$[M + H]^+$	289.0706	289.0707	0.13	153.0184, 163.0391	0.09 ± 0.01
5	Kaempferol 3-rutinoside	18.51	$C_{27} H_{30} O_{15}$	$[M + H]^+$	595.1657	595.1671	2.28	287.0552	0.52 ± 0.01
6	Quercetin	19.69	$C_{15} H_{10} O_7$	$[M\text{-}H]^-$	301.0353	301.0352	−0.63		0.11 ± 0.01
7	Azelaic acid	19.80	$C_9 H_{16} O_4$	$[M\text{-}H]^-$	187.0975	187.0973	−1.29	125.0970	1.14 ± 0.02
8	Neoeriocitrin	20.07	$C_{27} H_{32} O_{15}$	$[M\text{-}H]^-$	595.1668	595.1662	−1-12	151.0034, 135.0450, 459.1141	2.66 ± 0.03
9	Naringin	20.25	$C_{27} H_{32} O_{14}$	$[M + H]^+$	581.1864	581.1875	1.70	273.0755, 153.0182	0.11 ± 0.01
10	Naringenin 7 glucoside	20.29	$C_{21} H_{22} O_{10}$	$[M + H]^+$	435.1285	435.1291	1.24	273.0757, 153.0183	1.13 ± 0.01
11	Naringenin	20.30	$C_{15} H_{12} O_5$	$[M + H]^+$	273.0757	273.0757	−0-13	153.0183, 147.0442	24.58 ± 0.03
12	Hesperidin	21.83	$C_{28} H_{34} O_{15}$	$[M + H]^+$	611.1970	611.1980	1.57	303.0861, 153.0182	3.71 ± 0.02
13	Hesperetin	21.87	$C_{16} H_{14} O_6$	$[M + H]^+$	303.0863	303.0863	0	177.0547, 153.0183	46.70 ± 0.03
14	Hesperetin 7 glucoside	22.06	$C_{22} H_{24} O_{11}$	$[M + H]^+$	465.1391	465.1398	1.49	303.0864, 177.0548, 153.0184	3.89 ± 0.01

oxidative stability.

Fig. 2 (A) shows the characteristic heat flow trace over time obtained from the oxidation of linseed oil microparticles. The oxygen consumption was then calculated from the heat flow (as described in section 2.6) and is presented in Fig. 2 (B). Initially, the change in the oxygen concentration was minimal due to the protective effect of the wall material, which limited the oxygen contact with the oil. Additionally, the phenolic compounds in the orange flower extract acted as antioxidants by stabilizing the oxidation reaction. The rate of oxygen consumption during this phase is referred to as the rate of inhibition (R_{inh}).

As the protective barrier of the wall material degraded due to oxygen diffusion, and the antioxidants were gradually consumed by radicals, the rate of oxygen consumption increased. This marks the transition from the inhibited to the uninhibited period, during which the rate of oxygen consumption is defined as the rate of uninhibition (R_{uni}). The time required for this shift is called induction time (τ). A longer induction time indicates greater oxidative stability.

3.3.1. *Effect of C. aurantium flower extracts*

The efficiency of both the polar and apolar *C. aurantium* flower extracts at different concentrations (1, 2, and 5 mg/g of oil) was tested for enhancing the oxidative stability of linseed oil microparticles. Fig. 3 presents the heat flow and the corresponding oxygen consumption traces, which were used to determine the induction times (τ), and the rates of the inhibited (R_{inh}) and uninhibited (R_{uni}) periods. The kinetic parameters are summarized in Table 4. Encapsulated linseed oil

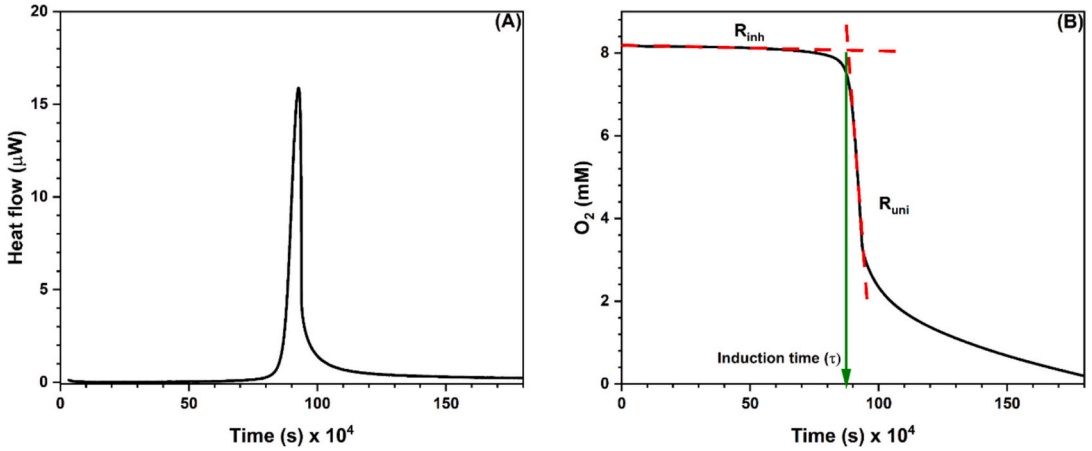

Fig. 2. Representative calorimetric trace of co-encapsulated linseed oil with *Citrus aurantium* L. *Subsp. Amara L.* flower extract. (A), heat flow vs. time trace; (B), oxygen consumption vs. time derived from the heat flow data.

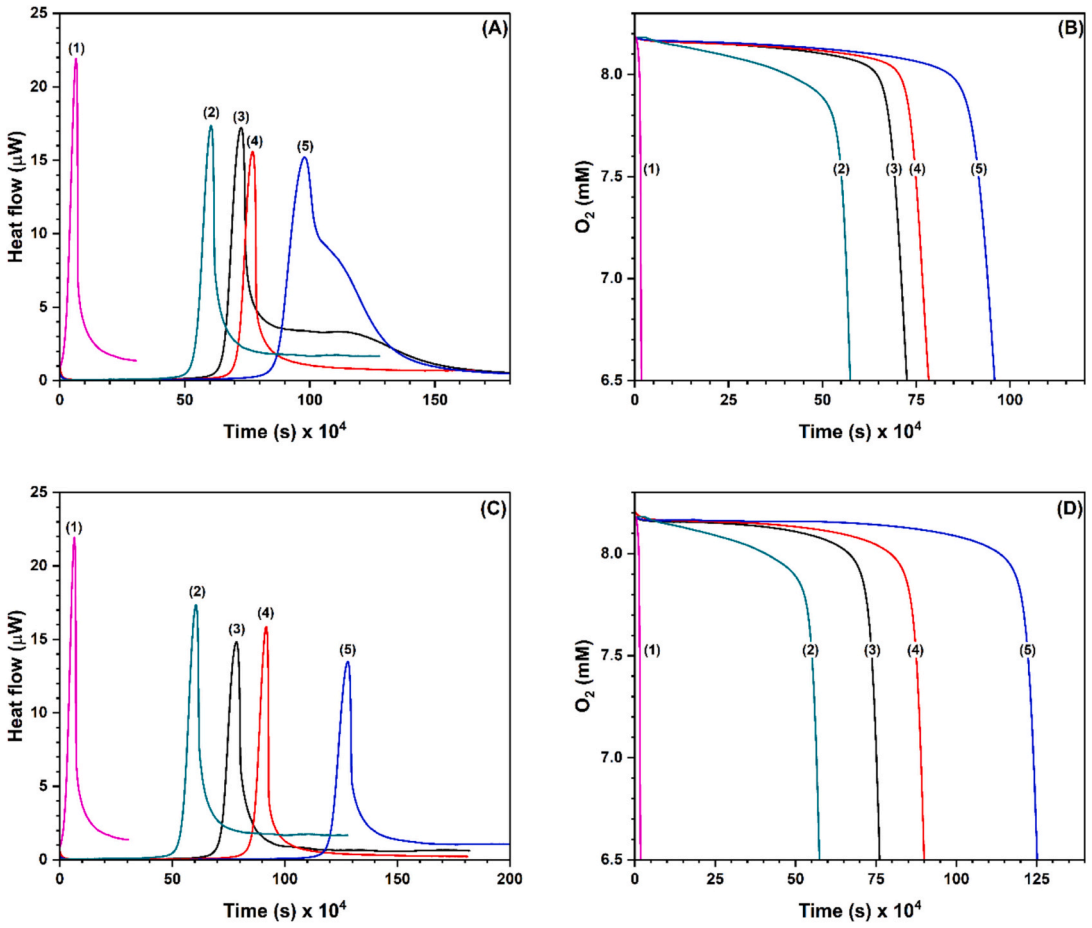

Fig. 3. Oxidative stability of bulk linseed oil and microparticles: heat flow (A, C) and oxygen consumption curves (B, D). A and B report data for apolar extracts, while C and D show results for polar extracts. Bulk linseed oil (1), encapsulated linseed oil (2), and linseed oil microparticles formulated with increasing concentrations of *Citrus aurantium* L. *Subsp. Amara L.* flower extracts at different concentrations: 1 m/g (3), 2 mg/g (4), and 5 mg/g of oil (5).

exhibited a significant increase ($p < 0.05$) in τ compared to bulk oil. These results confirmed the effectiveness of the encapsulation process in protecting the oil by limiting oxygen contact and improving the oxidative stability, consistent with the results reported by Le Priol et al. (2021). Furthermore, the incorporation of both *C. aurantium* flower extracts further increased the induction times (Table 4), following a linear trend with the concentration ($R^2 = 0.99$) for both extracts. At equivalent concentration, the polar extract showed a longer induction time compared to the apolar extract, which can be attributed to its higher TPC value.

Additionally, the incorporation of both extracts led to a significantly ($p < 0.05$) lower R_{inh} compared to the encapsulated linseed oil alone. At equivalent concentrations, the polar extract reported a lower R_{inh} than the apolar extract. For both the extracts, increasing the concentration

Table 4
Autoxidation kinetic parameters of PGSS encapsulated linseed oil derived from isothermal calorimetry data.

Sample	Extract	Induction time τ	R_{inh}	R_{uni}	*A.E*	k_{inh}
	(mg/g of oil)	(10^4 s)	(10^{-10} M·s^{-1})	(10^{-7} M·s^{-1})	(10^2)	(10^4 M^{-1}·s^{-1})
Bulk linseed oil	–	1.41 ± 0.33^{f}	229.6 ± 2.75^{a}	2.85 ± 0.06^{a}	–	–
Encapsulated linseed oil	–	55.11 ± 1.97^{e}	21.61 ± 0.98^{bc}	2.85 ± 0.08^{a}	–	–
Encapsulated linseed oil and apolar extract	1	68.51 ± 0.84^{d}	14.89 ± 1.13^{cd}	2.75 ± 0.01^{a}	5.20 ± 0.07^{c}	8.73 ± 0.07^{c}
	2	73.63 ± 1.13^{d}	13.70 ± 0.56^{cd}	2.75 ± 0.02^{a}	5.28 ± 0.02^{c}	8.85 ± 0.03^{c}
	5	92.37 ± 1.55^{c}	11.32 ± 0.42^{de}	2.79 ± 0.01^{a}	5.15 ± 0.08^{c}	8.76 ± 0.03^{c}
Encapsulated linseed oil and polar extract	1	75.70 ± 2.26^{d}	7.28 ± 0.02^{ef}	2.66 ± 0.03^{a}	9.72 ± 0.04^{a}	15.81 ± 0.02^{a}
	2	87.18 ± 2.40^{c}	6.33 ± 0.01^{ef}	2.67 ± 0.11^{a}	9.65 ± 0.02^{a}	15.70 ± 0.03^{a}
	5	123.12 ± 2.82^{a}	4.44 ± 0.01^{f}	2.57 ± 0.08^{a}	9.76 ± 0.01^{a}	15.22 ± 0.05^{a}
Encapsulated linseed oil and apolar + polar extract	2.5 + 2.5	111.46 ± 3.14^{b}	6.03 ± 0.08^{ef}	2.61 ± 0.16^{a}	7.91 ± 0.02^{b}	12.42 ± 0.04^{b}
Encapsulated linseed oil and BHT (200 μg/g)	–	117.53 ± 2.36^{ab}	18.33 ± 0.65^{bc}	2.52 ± 0.24^{a}	2.47 ± 0.01^{d}	3.75 ± 0.02^{d}

τ: induction time; R_{inh}: rate of oxidation during inhibited period; R_{uni}: rate of oxidation during uninhibited period; *A.E*: antioxidant efficiency; k_{inh}: inhibition rate constant.

resulted in a decrease of the R_{inh} indicating a dose-dependent effect. The R_{inh} parameter evaluates how well antioxidants can slow down the oxidation process. A lower R_{inh} value signifies strong inhibition of oxidation, whereas a higher value indicates weaker antioxidant activity and faster oil degradation (Suhag, Razem, et al., 2024). These findings are further supported by the results of the stopped-flow DPPH kinetic analysis, which demonstrated a higher rate constant for the polar extract leading to a faster neutralization of the DPPH radicals by antioxidants.

3.3.2. Antioxidant efficiency

Antioxidant efficiency (*A.E.*) is a valuable tool for quantitatively evaluating the effects of antioxidants in inhibiting autoxidation reactions. With an initiation rate of radical formation (R_i, eq. 7) equal to 9.5 × 10^{-11} M.s^{-1} the determination of the rate of the uninhibited period (R_{uni}) enabled the calculation of the oxidizability index (*O.I.*, eq. 11), which was found to be 5.11 × 10^{-2} M$^{-1/2}$ s$^{-1/2}$. Knowing the *O.I.*, and considering the rate constant for the termination reaction ($2k_t$) 10^7 M^{-1} s^{-1} which is consistent across various oxidizable substrates (Baschieri et al., 2019), the propagation rate constant (k_p) was determined to be 158 ± 5 M^{-1} s^{-1}. The k_p value is influenced by the degree of unsaturation of fatty acids and increases linearly with the number of double bonds, reaching values as high as 236 M^{-1} s^{-1} for pure methyl linolenate at 30 °C (Valgimigli, 2023).

Using the calculated k_p and R_{inh} values, the antioxidant efficiency (*A.E.*, using eq. 15) and the inhibited rate constant (k_{inh}) were determined (Table 4**)**. Notably, the *A.E.* of co-encapsulated linseed oil with the polar extract was approximately two times higher than that of the apolar extract. This difference in *A.E.* between the extracts can be attributed to their phytochemical composition as determined by HPLC-HRMS. The polar extract contained mainly flavonoids, whereas the apolar extract had a higher amount of alkaloids. While both flavonoids and alkaloids possess antioxidant properties, flavonoids tend to demonstrate more consistent and potent activity, as reported in other studies (Ahmad et al., 2024; Effiong et al., 2024). Moreover, the k_{inh} values for both the polar and apolar extract, as shown in Table 4, exhibited a similar trend to the rate constants determined using the stopped-flow DPPH kinetic method (Table 1). This observation supports the idea that the phytochemicals present in the polar extract are more efficient in trapping radicals, even when evaluated using different methods and conditions.

3.3.3. Additive effect of apolar and polar extracts

Interestingly, when the two extracts were added to the formulation at a concentration of 2.5 mg/g each, an additive effect was observed (Table 4**)**. The mixture reported a longer induction time compared to the one obtained from the apolar extract alone (5 mg/g), but shorter than that of the polar extract (Supporting information, Fig S3). These results suggest that the antioxidant properties of the two extracts can be tuned effectively when combined, enhancing the oxidative stability of linseed oil microparticles.

Additionally, this finding highlights the potential to tailor the antioxidant activity of *C. aurantium* flower extracts by adjusting the polarity of the extraction solvent. For example, incorporating a co-solvent like ethanol in SC-CO_2 extraction could enhance the antioxidant activity of the resulting extract, thereby improving its effect on the oxidative stability of different food products.

3.3.4. Comparison of polar and apolar extracts with synthetic antioxidant

Fig. 4 compares the oxidative stability of linseed oil microparticles prepared with BHT (200 μg/g) and equal concentrations (5 mg/g) of both the polar and apolar extracts. The microparticles containing BHT showed a longer induction period compared to the apolar extract, but shorter than the one obtained with the polar extract**.** Although BHT reported a longer induction time than the apolar fraction, the latter exhibited a significantly ($p < 0.05$) lower R_{inh}. This indicates that the antioxidant compounds present in the apolar extract were more effective in inhibiting the propagation of the oxidation process leading to higher *A.E.* In contrast, the polar extract outperformed both BHT and the apolar extract across all measured parameters, including a longer induction time, lower R_{inh}, and higher *A.E.* Furthermore, the combination of both the polar and apolar extracts (2.5 mg/g each) showed ~3 times higher *A.E.* compared to BHT in inhibiting the oxidation of linseed microparticles. Overall, these results provide evidence for the potential of *C. aurantium* flowers as a natural source of antioxidants, offering a promising alternative to synthetic options for use in food products.

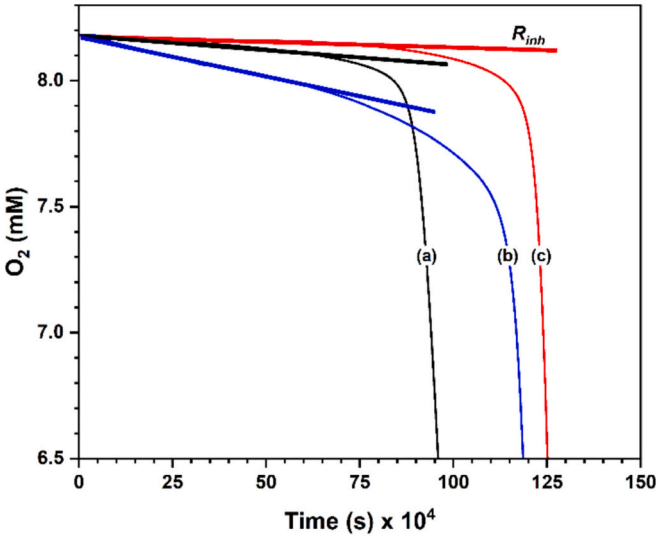

Fig. 4. Oxygen consumption of co-encapsulated linseed oil with (**a**) apolar extract (5 mg/g); (**b**) BHT (200 μg/g); and (**c**) polar extract (5 mg/g).

4. Conclusion

In conclusion, this study successfully valorised *C. aurantium* flowers through a sequential extraction process employing two green extraction techniques. The resulting extracts exhibited distinct phytochemical profiles, with the polar fraction showing higher phenolic content and superior antioxidant activity. When incorporated into linseed oil microparticles, both extracts significantly enhanced the oil's oxidative stability, with the polar fraction proving to be more effective than the apolar one. Notably, both extracts outperformed the synthetic antioxidant BHT, highlighting their potential as natural alternatives for enhancing the oxidative stability of oil-based products. Additionally, isothermal calorimetry proved to be a valuable tool for the real-time monitoring of the oxidative stability of linseed oil microparticles without the need for additional extraction steps. This technique effectively evaluated the antioxidant efficiency of various formulations in the presence of an oxidizable substrate, offering valuable insights into the application of green extraction techniques and the potential of natural antioxidants derived from orange flowers in food preservation.

While this study focused on the thermal stability of microparticles at 40 °C, future research could explore the extract's behaviour at higher temperatures, such as those used in cooking (80–100 °C) and frying (180 °C), to assess their stability and efficacy in food processing. Moreover, beyond the extracted bioactive fractions, the residual cake from both apolar and polar extractions may still contain valuable compounds, including fibers, residual phenolics, and other bioactives. Investigating its composition and potential applications could further enhance the sustainable utilization of *C. aurantium* flowers in food and pharmaceutical industries.

CRediT authorship contribution statement

Abdessamie Kellil: Writing – original draft, Methodology, Investigation, Formal analysis, Data curation, Conceptualization. **Rajat Suhag:** Investigation, Data curation. **Maria Concetta Tenuta:** Investigation, Data curation. **Sara Bolchini:** Investigation, Data curation. **Vakare Merkyte:** Investigation. **Matteo Scampicchio:** Writing – review & editing, Investigation, Formal analysis. **Ksenia Morozova:** Investigation. **Giovanna Ferrentino:** Writing – review & editing, Writing – original draft, Investigation, Data curation, Conceptualization.

Declaration of competing interest

The authors declare that they have no known competing financial interests or personal relationships that could have appeared to influence the work reported in this paper.

Acknowledgement

The authors would like to acknowledge the following awarded project: code PE00000003, Concession Decree No. 1550 of 11 October 2022 adopted by the Italian Ministry of University and Research, CUP D93C22000890001, Project title "ON Foods – Research and innovation network on food and nutrition Sustainability, Safety and Security – Working ON Foods". Project funded under the National Recovery and Resilience Plan (NRRP), Mission 4 Component 2 Investment 1.3 – Call for tender No. 341 of 15 March 2022 of Italian Ministry of University and Research funded by the European Union – NextGenerationEU.

Appendix A. Supplementary data

Supplementary data to this article can be found online at https://doi.org/10.1016/j.fochx.2025.102448.

Data availability

Data will be made available on request.

References

Ahmad, I., Huang, P.-J., Malak, N., Khan, A., Asad, F., & Chen, C.-C. (2024). Antioxidant potential of alkaloids and polyphenols of Viola canescens wall using in vitro and in silico approaches. *Frontiers in Chemistry, 12*. https://doi.org/10.3389/fchem.2024.1379463

Allay, A., Benkirane, C., Ben Moumen, A., Rbah, Y., Fauconnier, M.-L., Caid, H. S., … Mansouri, F. (2024). Enhancing bioactive compound extractability and antioxidant properties in hemp seed oil using a ternary mixture approach of polar and non-polar solvents. *Industrial Crops and Products, 219*, Article 119090. https://doi.org/10.1016/j.indcrop.2024.119090

Angeli, L., Morozova, K., & Scampicchio, M. (2023). A kinetic-based stopped-flow DPPH• method. *Scientific Reports, 13*(1), 1–8. https://doi.org/10.1038/s41598-023-34382-7

Baschieri, A., Pizzol, R., Guo, Y., Amorati, R., & Valgimigli, L. (2019). Calibration of squalene, p-cymene, and sunflower oil as standard Oxidizable substrates for quantitative antioxidant testing. *Journal of Agricultural and Food Chemistry, 67*(24), 6902–6910. https://doi.org/10.1021/acs.jafc.9b01400

Benzie, I. F. F., & Strain, J. J. (1996). The ferric reducing ability of plasma (FRAP) as a measure of "antioxidant power": The FRAP assay. *Analytical Biochemistry*. https://doi.org/10.1006/abio.1996.0292

Brand-Williams, W., Cuvelier, M. E., & Berset, C. (1995). Use of a free radical method to evaluate antioxidant activity. *LWT - Food Science and Technology, 28*(1), 25–30. https://doi.org/10.1016/S0023-6438(95)80008-5

Charles, D. J. (2013). Antioxidant properties of spices, herbs and other sources. In *Springer 4*. New York: Springer. https://doi.org/10.1007/978-1-4614-4310-0.

Chen, G.-L., Chen, S.-G., Xie, Y.-Q., Chen, F., Zhao, Y.-Y., Luo, C.-X., & Gao, Y.-Q. (2015). Total phenolic, flavonoid and antioxidant activity of 23 edible flowers subjected to in vitro digestion. *Journal of Functional Foods, 17*, 243–259. https://doi.org/10.1016/j.jff.2015.05.028

Cosgrove, J. P., Church, D. F., & Pryor, W. A. (1987). The kinetics of the autoxidation of polyunsaturated fatty acids. *Lipids, 22*(5), 299–304. https://doi.org/10.1007/BF02533996

Daud, N. M., Putra, N. R., Jamaludin, R., Md Norodin, N. S., Sarkawi, N. S., Hamzah, M. H. S., … Md Salleh, L. (2022). Valorisation of plant seed as natural bioactive compounds by various extraction methods: A review. *In Trends in Food Science and Technology*. https://doi.org/10.1016/j.tifs.2021.12.010

Degirmenci, H., & Erkurt, H. (2020). Chemical profile and antioxidant potency of Citrus aurantium L. flower extracts with antibacterial effect against foodborne pathogens in rice pudding. *LWT, 126*, Article 109273. https://doi.org/10.1016/j.lwt.2020.109273

Değirmenci, H., & Erkurt, H. (2020). Relationship between volatile components, antimicrobial and antioxidant properties of the essential oil, hydrosol and extracts of Citrus aurantium L. flowers. *Journal of Infection and Public Health, 13*(1), 58–67. https://doi.org/10.1016/j.jiph.2019.06.017

Effiong, M. E., Umeokwochi, C. P., Afolabi, I. S., & Chinedu, S. N. (2024). Comparative antioxidant activity and phytochemical content of five extracts of Pleurotus ostreatus (oyster mushroom). *Scientific Reports*. https://doi.org/10.1038/s41598-024-54201-x

Farag, M. A., Abib, B., Ayad, L., & Khattab, A. R. (2020). Sweet and bitter oranges: An updated comparative review of their bioactives, nutrition, food quality, therapeutic merits and biowaste valorization practices. *Food Chemistry, 331*, Article 127306. https://doi.org/10.1016/j.foodchem.2020.127306 (March).

Farhoosh, R. (2022). New insights into the kinetic and thermodynamic evaluations of lipid peroxidation. *Food Chemistry, 375*, Article 131659. https://doi.org/10.1016/j.foodchem.2021.131659 (August 2021).

Ferrentino, G., Morozova, K., Mosibo, O. K., Ramezani, M., & Scampicchio, M. (2018). Biorecovery of antioxidants from apple pomace by supercritical fluid extraction. *Journal of Cleaner Production*. https://doi.org/10.1016/j.jclepro.2018.03.165

Freeman, B. L., Eggett, D. L., & Parker, T. L. (2010). Synergistic and antagonistic interactions of phenolic compounds found in navel oranges. *Journal of Food Science*. https://doi.org/10.1111/j.1750-3841.2010.01717.x

Gasparini, A., Ferrentino, G., Angeli, L., Morozova, K., Zatelli, D., & Scampicchio, M. (2023). Ultrasound assisted extraction of oils from apple seeds: A comparative study with supercritical fluid and conventional solvent extraction. *Innovative Food Science and Emerging Technologies*. https://doi.org/10.1016/j.ifset.2023.103370

Gil-Martín, E., Forbes-Hernández, T., Romero, A., Cianciosi, D., Giampieri, F., & Battino, M. (2022). Influence of the extraction method on the recovery of bioactive phenolic compounds from food industry by-products. *Food Chemistry, 378*. https://doi.org/10.1016/j.foodchem.2021.131918

Guo, Y., Baschieri, A., Amorati, R., & Valgimigli, L. (2021). Synergic antioxidant activity of γ-terpinene with phenols and polyphenols enabled by hydroperoxyl radicals. *Food Chemistry, 345*, Article 128468. https://doi.org/10.1016/j.foodchem.2020.128468

Jokić, S., Rajić, M., Bilić, B., & Molnar, M. (2016). Supercritical extraction of Scopoletin from Helichrysum italicum (Roth) G. Don flowers. *Phytochemical Analysis, 27*(5), 290–295. https://doi.org/10.1002/pca.2630

Klein, E. J., Náthia-Neves, G., Vardanega, R., Meireles, M. A. A., da Silva, E. A., & Vieira, M. G. A. (2019). Supercritical CO2 extraction of A−/B-amyrin from uvaia (Eugenia pyriformis Cambess.): Effects of pressure and CO-solvent addition. *Journal of Supercritical Fluids, 153*, 1–6. https://doi.org/10.1016/j.supflu.2019.104595

Klettenhammer, S., Ferrentino, G., Imperiale, S., Segato, J., Morozova, K., & Scampicchio, M. (2023). Oxidative stability by isothermal calorimetry of solid lipid

microparticles produced by particles from gas saturated solutions technique. *Lwt, 173*, Article 114370. https://doi.org/10.1016/j.lwt.2022.114370 (August 2022).
Le Priol, L., Gmur, J., Dagmey, A., Morandat, S., El Kirat, K., Saleh, K., & Nesterenko, A. (2021). Co-encapsulation of vegetable oils with phenolic antioxidants and evaluation of their oxidative stability under long-term storage conditions. *Lwt, 142*, 1–6. https://doi.org/10.1016/j.lwt.2021.111033. February.
Lefebvre, T., Destandau, E., & Lesellier, E. (2021). Selective extraction of bioactive compounds from plants using recent extraction techniques: A review. *Journal of Chromatography A, 1635*, Article 461770. https://doi.org/10.1016/j.chroma.2020.461770
Legua, P., Modica, G., Porras, I., Conesa, A., & Continella, A. (2022). Bioactive compounds, antioxidant activity and fruit quality evaluation of eleven blood orange cultivars. *Journal of the Science of Food and Agriculture*. https://doi.org/10.1002/jsfa.11636
Li, J., Luo, Y., Zhan, L., Gu, Y., Zhang, W., Wen, Q., Feng, Y., & Tan, T. (2022). Comprehensive chemical profiling of the flowers of Citrus aurantium L. var. amara Engl. and uncovering the active ingredients of lipid lowering. *Journal of Pharmaceutical and Biomedical Analysis, 211*, Article 114621. https://doi.org/10.1016/j.jpba.2022.114621
Nabavi, S. F., Nabavi, S. M., & Ebrahimzadeh, M. A. (2016). *Antioxidant activity of hydro-alcoholic extracts of 4 citrus species flower. 18* pp. 74–80).
Ogunro, O. B., Richard, G., Izah, S. C., Ovuru, K. F., Babatunde, O. T., & Das, M. (2024). *Citrus aurantium: Phytochemistry, therapeutic potential, safety considerations, and research needs* (pp. 1–40). https://doi.org/10.1007/978-3-031-21973-3_69-1
Park, J. H., Lee, M., & Park, E. (2014). Antioxidant activity of orange flesh and peel extracted with various solvents. *Preventive Nutrition and Food Science, 19*(4), 291–298. https://doi.org/10.3746/pnf.2014.19.4.291
Pereira, M. G., Maciel, G. M., Haminiuk, C. W. I., Bach, F., Hamerski, F., de Paula Scheer, A., & Corazza, M. L. (2019). *Effect of extraction process on composition, antioxidant and antibacterial activity of oil from yellow passion fruit (Passiflora edulis Var. Flavicarpa) seeds. Waste and biomass valorization*. https://doi.org/10.1007/s12649-018-0269-y
Pryor, W. A., Cornicelli, J. A., Devall, L. J., Tait, B., Trivedi, B. K., Witiak, D. T., & Wu, M. (1993). A rapid screening test to determine the antioxidant potencies of natural and synthetic antioxidants. *Journal of Organic Chemistry, 58*(13), 3521–3532. https://doi.org/10.1021/jo00065a013
Rahmania, H., Kato, S., Sawada, K., Hayashi, C., Hashimoto, H., Nakajima, S., Otoki, Y., Ito, J., & Nakagawa, K. (2020). Revealing the thermal oxidation stability and its mechanism of rice bran oil. *Scientific Reports, 10*(1), 1–11. https://doi.org/10.1038/s41598-020-71020-y
Reis, D. R., Ambrosi, A., & Luccio, M. D. (2022). Encapsulated essential oils: A perspective in food preservation. *Future Foods, 5*, Article 100126. https://doi.org/10.1016/j.fufo.2022.100126 (August 2021).
Shehzad, Q., Rehman, A., Jafari, S. M., Zuo, M., Khan, M. A., Ali, A., … Xia, W. (2021). Improving the oxidative stability of fish oil nanoemulsions by co-encapsulation with curcumin and resveratrol. *Colloids and Surfaces B: Biointerfaces, 199*, Article 111481. https://doi.org/10.1016/j.colsurfb.2020.111481
Siger, A., Nogala-Kalucka, M., & Lampart-Szczapa, E. (2008). The content and antioxidant activity of phenolic compounds in cold-pressed plant oils. *Journal of Food Lipids*. https://doi.org/10.1111/j.1745-4522.2007.00107.x
Singleton, V. L., & Rossi, J. A. (1965). Colorimetry of Total Phenolics with Phosphomolybdic-Phosphotungstic acid reagents. *American Journal of Enology and Viticulture, 16*(3), 144–158. https://doi.org/10.5344/ajev.1965.16.3.144
de Sousa, D. P., Damasceno, R. O. S., Amorati, R., Elshabrawy, H. A., de Castro, R. D., Bezerra, D. P., … Lima, T. C. (2023). Essential oils: Chemistry and pharmacological activities. *In Biomolecules*. https://doi.org/10.3390/biom13071144
Suhag, R., Ferrentino, G., Morozova, K., Zatelli, D., Scampicchio, M., & Amorati, R. (2024). Antioxidant efficiency and oxidizability of mayonnaise by oximetry and isothermal calorimetry. *Food Chemistry, 433*, Article 137274. https://doi.org/10.1016/j.foodchem.2023.137274 (August 2023).
Suhag, R., Kellil, A., Ferrentino, G., Morozova, K., Zatelli, D., & Scampicchio, M. (2025). Lipid oxidation kinetics and antioxidant efficiency in foods using isothermal calorimetry. *Trends in Food Science & Technology, 155*, Article 104801. https://doi.org/10.1016/j.tifs.2024.104801
Suhag, R., Razem, M., Ferrentino, G., Morozova, K., Zatelli, D., & Scampicchio, M. (2024). Real-time monitoring of vegetable oils photo-oxidation kinetics using differential photocalorimetry. *Food Chemistry, 456*, Article 140011. https://doi.org/10.1016/j.foodchem.2024.140011
Valgimigli, L. (2023). Lipid peroxidation and antioxidant protection. *Biomolecules, 13*(9). https://doi.org/10.3390/biom13091291
Villeneuve, P., Bourlieu-Lacanal, C., Durand, E., Lecomte, J., McClements, D. J., & Decker, E. A. (2023). Lipid oxidation in emulsions and bulk oils: A review of the importance of micelles. *Critical Reviews in Food Science and Nutrition, 63*(20), 4687–4727. https://doi.org/10.1080/10408398.2021.2006138
Wang, Y., Liu, X. J., Chen, J. B., Cao, J. P., Li, X., & Sun, C. D. (2022). Citrus flavonoids and their antioxidant evaluation. *In Critical Reviews in Food Science and Nutrition*. https://doi.org/10.1080/10408398.2020.1870035
Xiao, S., & Ahn, D. U. (2023). Co-encapsulation of fish oil with essential oils and lutein/curcumin to increase the oxidative stability of fish oil powder. *Food Chemistry, 410*, Article 135465. https://doi.org/10.1016/j.foodchem.2023.135465 (October 2022).
Zhang, X., Zhuang, X., Xiong, T., Huang, S., Qian, X., Guo, T., Chen, M., Xie, W., & Huang, Y. (2023). Extraction from different parts of Citrus maxima flowers using ultrasound as an aid and study of their composition and function. *Ultrasonics Sonochemistry, 100*, Article 106632. https://doi.org/10.1016/j.ultsonch.2023.106632 (September).